Fusion, transfer and total reaction cross sections at sub- and near-barrier energies of the ^{6}Li+^{28}Si system

A. Pakou*,[1] K. Rusek,[2] N. Alamanos,[3] X. Aslanoglou,[1] M. Kokkoris,[4] A. Lagoyannis,[5] T. J. Mertzimekis,[1] A. Musumarra,[6] N. G. Nicolis,[1] D. Pierroutsakou,[7] and D. Roubos[1]

[1] *Department of Physics, The University of Ioannina, 45110 Ioannina, GREECE*

[2] *Department of Nuclear Reactions, The Andrzej Sołtan Institute for Nuclear Studies, Hoża 69, 00-681 Warsaw, POLAND*

[3] *DSM/DAPNIA CEA SACLAY, 91191 Gif-sur-Yvette, FRANCE*

[4] *National Technical University of Athens-GREECE*

[5] *National Research Center Demokritos-GREECE*

[6] *Dipartimento di Metodologie Fisiche e Chimiche per l'Ingegneria dell'Universita di Catania, ITALY*

[7] *INFN Sezione di Napoli, I-80125, Napoli, ITALY*

(Dated: July 4, 2008)

Abstract

Total reaction cross section measurements with the γ-spectroscopy method and a detailed energy mapping of transfer versus total reaction cross section ratios, in exclusive particle-γ measurements, have been performed for ^{6}Li+^{28}Si at sub- and near-barrier energies with the aim of studing fusion. Large enhancements of the total reaction cross sections versus one barrier penetration calculations were observed and were attributed to a large transfer contribution. Fusion cross sections were deduced for the first time by subtracting total reaction and transfer cross sections and it was shown that even in the case of the weakly bound nucleus ^{6}Li interacting with a "simple" target like ^{28}Si, the fusion probability can be described adequately well within a one-dimensional barrier penetration framework.

PACS numbers: 25.70.Bc, 24.10.Ht, 24.10.Lx, 24.50.+g, 27.20.+n

* corresponding author, e-mail: apakou@cc.uoi.gr

Fusion, in a very simple approach, can be described by the tunnelling of two rigid spherical objects through their mutual interaction potential. In this context, one-dimensional barrier penetration models (BPM) were developed and applied to fusion data [1, 2]. Later, it was shown that couplings to internal degrees of freedom of the two colliding nuclei can dramatically modify the tunnelling probability, while direct channels like transfer may compete with fusion even at energies below the barrier [3, 4]. The observed reaction cross sections in this energy regime were found to be orders of magnitude larger than the BPM predictions [5, 6]. Also, the question of a possible correlation between transfer and fusion has been thoroughly investigated [7–10].

The subject of fusion, while not fully understood for stable nuclei, has been revisited with the advent of radioactive nuclear beam facilities. Studies are now concentrated on weakly-bound radioactive or stable projectiles in the expectation that the weakly bound nature of such projectiles affects greatly the reaction mechanism picture via the breakup and/or transfer channels [10, 11]. A major point of confusion however in interpreting fusion results emerged due to an assumption made in several measurements at sub- and near-barrier energies, where fusion is taken to be equal to the total reaction cross section. This is not true. As was inferred some years ago from inclusive α-production measurements [12–15] and finally from exclusive measurements [16–18], transfer is a dominant mechanism at sub- and near-barrier energies in these systems and accounts for most of the enhancement observed at sub- and near- barrier energies in the "fusion" cross sections compared to one-dimensional BPM calculations. We put fusion in quotation marks since several of the measurements of "fusion", for systems where direct and compound mechanisms lead to the same residual nuclei, are rather total reaction cross section measurements, as they can not distinguish between evaporation and transfer exit channels. Especially in singles measurements adopting the γ-spectroscopy method and extracting "fusion" cross sections by taking into account branching ratios via a compound theory rather than summing all the ground state transitions the measured cross sections can not really be quoted either as total reaction cross sections or as fusion cross sections. As is very well stated in [17], before interpreting results with weakly-bound projectiles it is very important to ensure that the quoted fusion cross sections do not contain contributions from other mechanisms.

In this spirit, we present in this letter total reaction cross sections at sub- and near-barrier energies with the γ-spectroscopy method and we attempt a detailed energy mapping

of transfer versus total reaction cross section ratios with transfer measurements and the aid of Continuum-Discretized Coupled Channels (CDCC) and CDCC+BPM calculations. Subsequently, we estimate the complete fusion cross sections for the system ^{6}Li+^{28}Si. The choice of the particular system facilitates our study since, as we demonstrated in [18], it is not affected by complications arising from incomplete fusion and breakup. Therefore, this system is the most suitable for unfolding the "enigma" of fusion by separating transfer from total reaction cross sections. We note that the total reaction cross section measurements at sub-barrier energies are performed for the first time while the near barrier cross section measurements give the opportunity of testing the method via comparisons with previously obtained values [19, 20].

Beams of $^{6}Li^{3+}$ were delivered by the TN11/25 HVEC 5.5 MV Tandem accelerator of the National Research Center of Greece-DEMOKRITOS at several bombarding energies from 6 to 16 MeV. Beam currents were of the order of 30 nA. The beam impinged on a 400 μg/cm^2 thick self supporting natural silicon target in a target frame fixed parallel to the face of the detector. Two types of measurements were performed: angular distributions in a particle-γ coincidence mode described previously in [18] and singles measurements, to deduce both transfer (at 8 and 15 MeV) and total reaction cross sections (between 6 to 16 MeV), respectively. Angular distributions were measured with two telescopes (ΔE=10μm, E=2000μm) set 12.7 cm from the target, rotated in a D-shape chamber, in the angular range θ_{lab}=20^0 to 70^0. Gamma rays were observed by a 50% efficient Ge detector, fixed at 90^0 with respect to the beam direction, 3.1 cm from the target. A coincidence requirement between particles and gammas allowed the clear identification of each channel and subsequently via evaporation calculations the determination of the transfer contribution for each channel. Singles gamma measurements were performed in the same setup, with the Ge detector at 90^0, using the elastically scattered lithium observed in the telescopes for normalisation purposes. The efficiency of the Ge detector was determined via a ^{152}Eu source of known activity. Summing effects were estimated by placing a ^{152}Eu and ^{22}Na source at various distances from the detector.

For each exit channel, in both singles and coincidence measurements, cross sections were obtained by summing up gammas from all ground state transitions. In the latter case, gammas were tagged with alpha and/or proton particles. These ground state transitions include gammas de-exciting the first and the higher excited states up to 3 and 6 MeV, depending on

channel and beam energy. Losses due to direct feeding of the ground state are estimated to be of the order of 2% according to compound calculations. These calculations were tested in this work against reaction channels which were formed purely via compound processes, while were also validated before [21, 22] via inclusive angular distribution measurements at more backward angles.

Total reaction cross sections were obtained by summing the cross sections of all the observed exit channels and the missing channels, the latter estimated via CASCADE calculations [23]. Missing channels lead to ^{32,31,30}P, with ^{32}P most prominent and do not exceed 20% to 30% of the measured cross section from lower to higher energies. Observed and therefore measured channels lead to : ^{29,28}Si, ^{32,33}S and ^{29}P. Our results are presented in Figure 1 and Table I. The sub-barrier total reaction cross sections are performed for the first time while the near barrier ones serve both for the systematic presentation of cross sections at sub- and near-barrier energies and for testing our method by comparisons with previous measurements. Therefore, in the same Figure previous results at near-barrier energies, obtained via elastic scattering on ^{28}Si [19] and ^{27}Al [24] and via direct measurements on ^{28}Si, are also presented and compared with the present results showing very good compatibility. It should be noted that the ^{27}Al results were analysed in the context of the present work in the same theoretical framework as previously for the ^{28}Si results [19]. Previous results [15] at E_{lab}=13, 20 and 25 MeV are also shown and are found in very good agreement with all the other values. The experimental results are also compared in Figure 1 with predictions generated by Continuum-Discretized Coupled-Channels calculations (CDCC) and are found to be in good agreement. To obtain reaction cross sections in this framework we note that the elastic scattering can be well reproduced by simple optical model calculations, where the effective ^{6}Li+^{28}Si potential is described as a sum of a bare and a dynamic polarisation potential. The bare potential is calculated by means of the single folding technique from alpha+target and d+target empirical optical model potentials. The dynamic polarisation potential, generated by the breakup of the lithium in the field of the silicon target, is derived from CDCC calculations following the prescription of Thompson et al. [25]. It is assumed that ^{6}Li has a simple two-body alpha+d cluster structure and couplings with the resonant and non-resonant states of alpha+d continuum are taken into account. The elastic scattering calculations based on this optical model reproduce very well the ^{6}Li+^{28}Si elastic scattering data [19] as well as breakup cross section data [26] with no free parameters. More

details of the calculation can be found in [26, 27]. Finally in the same Figure, Figure 1, we present BPM calculations according to Wong [28]. The total reaction cross section is greatly enhanced against this prediction by almost a factor of ∼80 % for E/V_b=0.8 to ∼20% beyond E/V_b=2.

Subsequently, having obtained total reaction cross sections, both theoretically and experimentally, our goal was twofold. First to identify and quantify transfer as a strong mechanism contributing even at sub-barrier energies, which gives the enhancement of the total reaction cross sections against BPM calculations, and second to estimate in an internally consistent way into the context of the present experiment, fusion cross sections. This could be visualised by obtaining a detailed energy mapping of the above ratio. Experimentally, the method to obtain a detailed energy mapping can give, in a straight forward way, fusion but it is very time consuming. Therefore, in this work we have performed transfer measurements at two energies, namely 8 and 15 MeV, complementing the results of [18] and then we tried to describe these results theoretically in order to obtain the necessary interpolations and/or extrapolations for a detailed energy mapping. In Figure 2 we present our angular distribution measurements at 15 MeV for the exit channels ^{29}Si+α+p (Q=+2.812MeV), ^{29}P+α+n (Q=-1.842 MeV) and ^{32}S+p+n (Q=+5.476 MeV) together with DWBA calculations obtained in a similar way to that presented in [27]. In the same figure "new" transfer data are also presented. These data were obtained following the method described in references [18, 21] ("new" datum at each angle = original datum at each angle minus the compound contribution for this angle calculated by the CASCADE code). Total transfer cross sections for each channel were obtained by integrating the angular distributions of the "new" data. Tabulated results for transfer and reaction cross sections are presented in Table II. Ratios of total transfer to total reaction cross section were formed and are presented in Figure 3. The energy variation of this ratio presents an increasing trend approaching the barrier. Below barrier this increase is strong and it will be desirable to trace the energy of transfer quenching. But this was unobtainable with the present experimental setup. In the same Figure we present the decomposition of the experimental ratios to ratios for each observed transfer channel (1n-transfer, 1p-transfer and 1α-transfer versus total reaction cross section). It is obvious that dominant channel appears to be the 1n-transfer one, while 1p-transfer contributes to a lesser extend and α-transfer contributes only at the higher energies. Subsequently we present previous results for ^{6}Li+^{28}Si [15] at E_{lab}= 13, 20 and 25 MeV and results for ^{9}Be+^{28}Si [15] at

E_{lab}= 14, 17, 20, 23 and 26 MeV. To present results with different projectiles in one Figure, we plot them as a function of E/V_b with barriers calculated according to Broglia [29], $V_b{}^{lab}$= 8.54 and 12 MeV for ^{6}Li and ^{9}Be correspondingly. For the previous results of ^{6}Li on silicon, it seems that the datum in the overlapping experimental region is in in very good agreement with our results while the higher energy data exhibit much higher values than the present calculations. We note however, that these measurements are inclusive measurements and may contain some impurity channel and/or breakup at the higher energies. On the other hand the results for ^{9}Be on silicon show the same increasing trend approaching sub-barrier energies while exhibiting constant values after E/V_b=1.5 as the present results of ^{6}Li. The observed difference in the strength between the ^{6}Li and ^{9}Be ratios may be attributed to the weaker nature of the second nucleus and variations in the Q-values of the two reactions.

To obtain calculated ratios of transfer versus reaction cross sections we have preferred to deduce the direct cross sections by subtracting reaction and fusion cross sections, since as seen in Figure 2 and also mentioned in [27], transfer DWBA calculations reproduce only the shape and not the magnitude of the data. Taking into account that breakup is negligible for this system [26], the direct part may be taken to be equal to transfer. In order to calculate the fusion cross section we applied a barrier penetration model (BPM). In this model the fusion cross section depends on the Coulomb barrier defined as the sum of the effective ^{6}Li+^{28}Si nuclear and Coulomb potentials. The effective nuclear potential was taken to be the sum of the bare potential and the dynamic polarisation potential. The bare potential was derived from empirical alpha+^{28}Si and d+^{28}Si optical model potentials and the cluster wave function of the ^{6}Li ground state by means of single folding technique while the dynamic polarisation potential was derived from CDCC calculations following the prescription of Thompson et al [25]. Results for the calculated ratios of transfer to reaction cross sections ($R_{theory}=(\sigma_{T(theory)}-\sigma_{F(theory)})/\sigma_{T(theory)}$) are compared with the experimental values in Figure 3. The calculated values are in very good agreement with our data, supporting the use of the calculated ratios in order to determine the fusion cross sections. The so estimated fusion cross sections ($\sigma_F=\sigma_{T(measured)}-\sigma_{T(measured)}*R_{theory}$) are therefore the calculated above $\sigma_{F(theory)}$ values, normalised to the measured and calculated total reaction cross section ($\sigma_F=\sigma_{F(theory)}*(\sigma_{T(measured)}/\sigma_{T(theory)})$

Our results for fusion are presented in Figure 4 and Table I. The assigned errors in the fusion cross sections are due to statistical uncertainties, the normalisation to the elastically

scattered lithium and the uncertainty in the thickness of the target, and do not exceed 10% of the cross section for the highest energies and 15 % for the lower ones. If, however, we introduce an additional uncertainty in the ratio R_{theory}, the estimated error in the fusion cross section is greatly increased at the lower energies and slightly increased at the higher energies, due to the different slope of the theoretical curve. For example, if we take a 10% error in R_{theory}, which corresponds to the theoretical curve which best fits the data, then the error is increased to 15% and 180% at the highest and lowest energies, respectively. In the same Figure we present also previous results of [15] at E_{lab}=13, 20, 25 MeV. These results show a lower trend than the present ones due to the higher estimation for the transfer contribution (see Figure 3). The experimental fusion results are compared with various BPM calculations in Figure 4: a) those described above, b) calculations according to Wong [28] and c) calculations according to our theory presented in [30]. In this last case, calculations were performed with the code ECIS [31]. The real part of the entrance potential was taken from our elastic scattering study [19] within the double folding model framework using the BDM3Y1 interaction developed by Khoa et al. [32] with a normalisation factor N=0.65. The imaginary potential was so arranged to absorb all the flux penetrating the barrier, simulating the ingoing wave boundary condition. Couplings to inelastic states of ^{28}Si and ^{6}Li were found to modify the results by not more than 3% and were not taken into account. As may be seen, the complete fusion data (total fusion, since incomplete fusion if present is negligible) can be well estimated by any BPM calculation especially when the used effective optical potential is validated via elastic scattering data. Moreover, the agreement of the ECIS calculations with the fusion experimental results, deduced by subtracting total reaction and transfer cross sections, points out the following very interesting conclusion. The reduction of the real potential for weakly bound nuclei, in this case described by a normalization factor of N=0.65, can be rather attributed to transfer and not to breakup as it is beleived by to day. Arguments of the reduction of the potential due to transfer was given previously in [14, 19] via our elastic scattering and α-production measurements on ^{6}Li+^{28}Si and now is fully validated into the context of the present work.

An interesting question which remains open after the completion of the present work concerns the energy evolution of the transfer versus reaction cross section ratios at very low energies and the energy position of transfer quenching, unobtainable with the present setup. Such measurements would be of great value for related topics in Astrophysical problems.

Summarising, we have obtained both experimentally and theoretically total reaction cross sections for ^{6}Li+^{28}Si at sub- and near barrier energies, namely at E_{lab}= 6 to 16 MeV. It was shown that these results are greatly enhanced against BPM calculations. We have quantify this enhancement which is proved to be due to a strong 1n-transfer channel and to a lesser extend due to 1p and 1α-transfer channels. The energy evolution of the enhancement, that is the ratio of direct to total reaction cross section was also obtained via exclusive particle -γ angular distribution measurements and the aid of CDCC calculations. Fusion cross sections were estimated during this procedure and were found to be very well described by BPM calculations especially when effective potentials are validated via elastic scattering measurements.

The main conclusion of this work is that, for weakly bound projectiles where compound and direct mechanisms lead to the same residual nuclei, fusion is not equal to total reaction cross section at sub and near-barrier energies. The reaction channels responsible for this "disagreement" are strong transfer channels which persist down to sub-barrier energies.

---

[1] C. Y. Wong, Phys. Rev. Lett. **31**, 766(1973).

[2] L. C. Vaz, J. M. Alexandez and G. R. Satchler, Phys. Rep. **69**, 373 (1981).

[3] M. Beckerman, Phys. Rep. **129**, 145 (1985).

[4] M. Dasgupta and D. J. Hinde, N. Rowley, A. M. Stefanini, Ann. Rev. Nucl. Part. Sci. **48**, 401 (1998).

[5] M. Beckerman et al., Phys. Rev. Lett. **45**, 1472(1980).

[6] J. R. Leigh et al., Phys. Rev. **C 52**, 3151(1995).

[7] L. Corradi, Proceeding of the Workshop : Heavy-Ion Fusion : exploring the variety of nuclear properties", eds. A.M.Stefanini et al. Padova, Italy, May 25-27, p.34 (1994).

[8] R. A. Broglia, C.H. Dasso, S. Landowne and A. Winter, Phys. Rev. **C 27**, R2433 (1983).

[9] W. Henning, F. L. H. Wolfs, J. P. Schiffer and K. E. Rehm, Phys. Rev. Lett. **58**, 318(1987).

[10] N. Keeley, R. Raabe, N. Alamanos, J. L. Sida, Prog. Part. and Nucl. Phys. **59**, 579(2007).

[11] L. F. Canto, P. R. S.Gomes, R. Donangelo, M. S. Hussein, Phys. Rep. **424**, 1 (2006).

[12] C. Signorini et al., Eur. Phys. J. **A10**, 249 (2001).

[13] A. F. Aguilera et al., Phys. Rev. Lett. **84**, 5058 (2000).

[14] A. Pakou et al., Phys. Rev. Lett. **90**, 202701 (2003).

[15] M. Hugi et al., Nucl. Phys. **A 368**, 173 (1981).

[16] A. Raabe et al., Nature (London) **431**, 823 (2004).

[17] A. Navin et al., Phys. Rev. **C 70**, 044601 (2004).

[18] A. Pakou et al., Phys. Rev. **C 76**, 054601 (2007).

[19] A. Pakou et al., Phys. Lett. **B 556**, 21 (2003).

[20] A. Pakou et al., Nucl. Phys. **A 784**, 13 (2007).

[21] A. Pakou et al., Phys. Rev. **C 71**, 064602 (2005).

[22] A. Pakou et al., Journal of Physics **G 31**, S1723 (2005).

[23] CASCADE: A Nuclear Evaporation Code, F. Puhlhofer, Nucl. Phys. **A280**, 267(1979); M. N. Harakeh extended version

[24] J. M. Figueira et al., Phys. Rev. **C 75**, 017602 (2007).

[25] I. J. Thompson et al. Nucl. Phys. **A 505**, 84 (1989).

[26] A. Pakou et al., Phys. Lett. **B 633**, 691 (2006).

[27] A. Pakou et al., Phys. Rev. **C 69**, 054602 (2004).

[28] C. Y. Wong, Phys. Rev. Lett. **31**, 766 (1973).

[29] Ricardo. A. Broglia and Aage. Winther, Heavy Ion Reactions, Volume I: Elastic and Inelastic Reactions; The Benjamin/ Cummings Publishing Company, Inc (1981).

[30] N. Alamanos et al., Phys. Rev. **C 65**, 054606 (2002).

[31] J. Raynal, Phys. Rev. **C 23**, 2571 (1981).

[32] D. T. Khoa et al., Phys. Lett. **B 342**, 6 (1995).

[33] K. Rusek, Phys. Rev. **C 70**, 014603 (2004).

$E_{c.m.}$ (MeV)	σ_T(mb)	σ_F(mb)
4.94	18 ± 3	2.3±0.4(4.3)
5.35	43 ± 7	8.6±1.4(9.6)
5.5	47 ± 5	11.3±1.4(8.3)
5.76	55 ± 6	17±2(8)
6.18	98 ± 10	42±4(13)
6.5	210 ± 21	107±11(26)
7.2	325 ± 33	211±22(37)
7.41	345 ± 35	238±24(38)
8.23	493 ± 50	375±38(53)
9.05	670 ±70	524±55(73)
10.54	930±100	730±80(103)
10.7	1000±120	800±96(124)
12.2	1112±122	890±98(126)
12.4	1168±130	934±104(135)
13.2	1300±150	1040±120(155)

TABLE I: Total reaction cross sections, σ_T, and fusion cross sections, σ_F. The quoted error on fusion cross sections is calculated according to the error assigned in the total reaction cross sections. The value in parentheses, gives the error in fusion cross sections, if we take into account a 10% uncertainty in the ratio of transfer versus total reaction. The energy, $E_{c.m.}$ refers to the projectile energy in the middle of the target

^{6}Li+^{28}Si$\rightarrow$	E_{lab}(MeV)	$\sigma_{T.C.}$(mb)	σ_E(mb)	$\sigma_D{}^{exp}$(mb)	$\sigma^{exp}{}_D/\sigma_E$
^{29}Si+α+p	15	480±72	328	172±72	0.52±0.21
	13	355±29	242	113±29	0.47±0.12
	9	177±10	70	107±10	1.53±0.13
	8	118±30	36	82±30	2.27±0.83
^{32}S+p+n	15	260±52	213	47±52	0.22 ±0.24
	13	270±15	232	38±15	0.16 ±0.06
	9	65±1	72	-	-
	8	26±5	28	-	-
^{29}P+α+n	15	52.4±11	12.4	40±11	3.3±0.9
	13	46±5	7	40±5	5.7±0.7
	9	21±1	1.67	21±1	12.6± 0.6
	8	22±13	1.26	20±13	15.9± 10

TABLE II: Observed, open channels in the reaction ^{6}Li+^{28}Si at beam energies 8, 9, 13 and 15 MeV populated both via a direct and compound procedure. Reaction cross sections for each channel (compound +direct), $\sigma_{T.C.}$, are obtained by integrating measured angular distributions of light particles in coincidence with gammas. Evaporation cross sections, σ_E, are calculated values via the code CASCADE (see text). Transfer cross sections, $\sigma_D{}^{exp}$, are values obtained by integration of the angular distribution "new data" (see text). Present results are the ones at 8 and 15 MeV while for reasons of completeness we present also previous results [18] at 9 and 13 MeV.

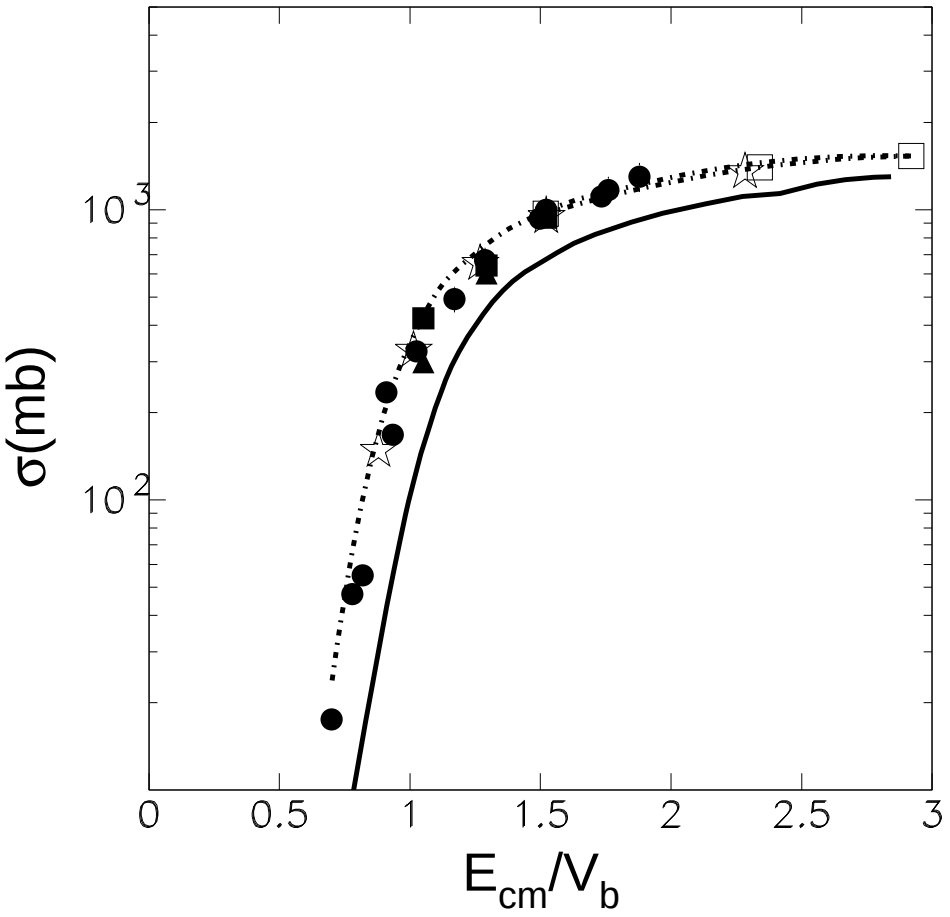

FIG. 1: Total cross sections as a function of energy versus the Coulomb barrier for ^{6}Li+^{28}Si. The present measurements are denoted by the solid circles, previous measurements from elastic scattering and direct reaction measurements [19, 20] by the solid squares and triangles, respectively. Previous measurements [24] for the system ^{6}Li+^{27}Al obtained from elastic scattering (see text), are denoted by open stars. Coulomb barriers in the centre of mass, V_b, were calculated according to Broglia [29] and are V_b=7.03 and 6.56 MeV for ^{6}Li+^{28}Si and ^{6}Li+^{27}Al, respectively. Optical model calculations, denoted by the dot-dashed line, compare well with the data. Previous results at 13 MeV -overlapping region with the present one- and at 20 and 25 MeV [15] are presented with open squares and show very good compatibility with the trend of the present results. The solid line represents BPM calculations according to Wong [28].

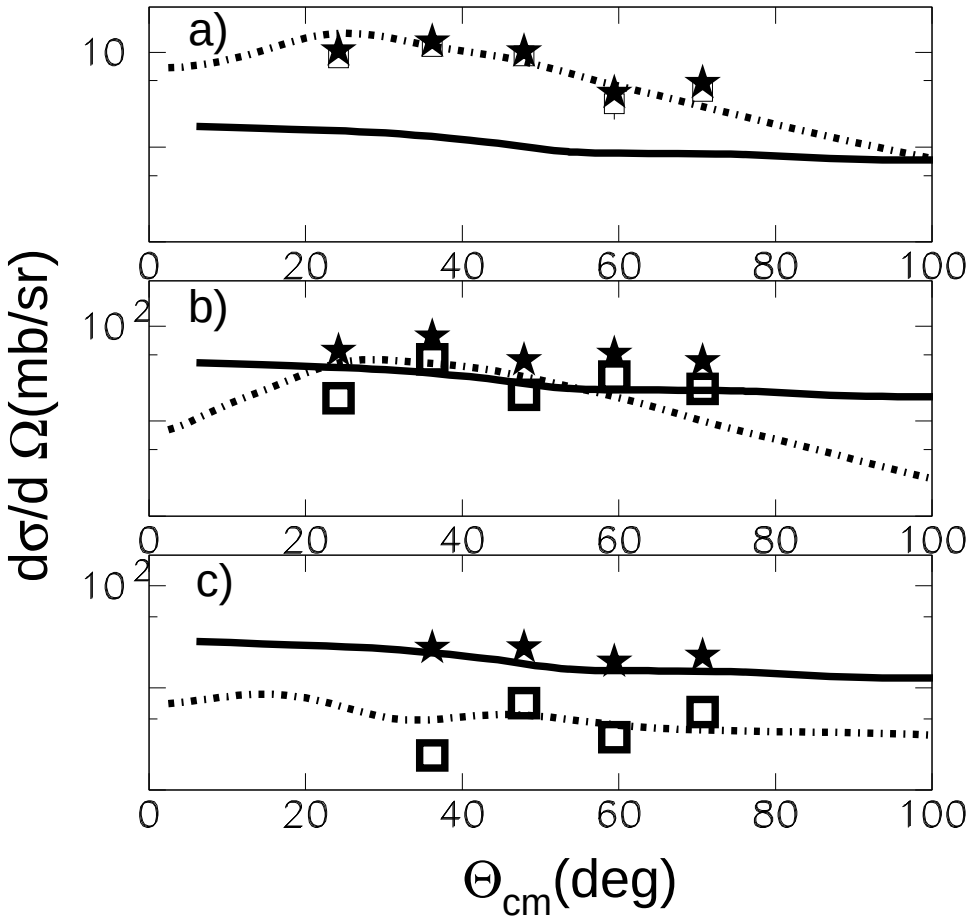

FIG. 2: Proton and alpha angular distributions for the ^{6}Li+^{28}Si exit channels at 15MeV: a) ^{29}P+ α+n, b) ^{29}Si+ α+p and c) ^{32}S+p+n. the data are denoted by the stars, "new" data with open cubes – see text. Solid lines are CASCADE calculations and dot-dashed lines are DWBA calculations. In case b) the DWBA calculation was multiplied by a factor of 3.5, while in case c) by a factor of 4.

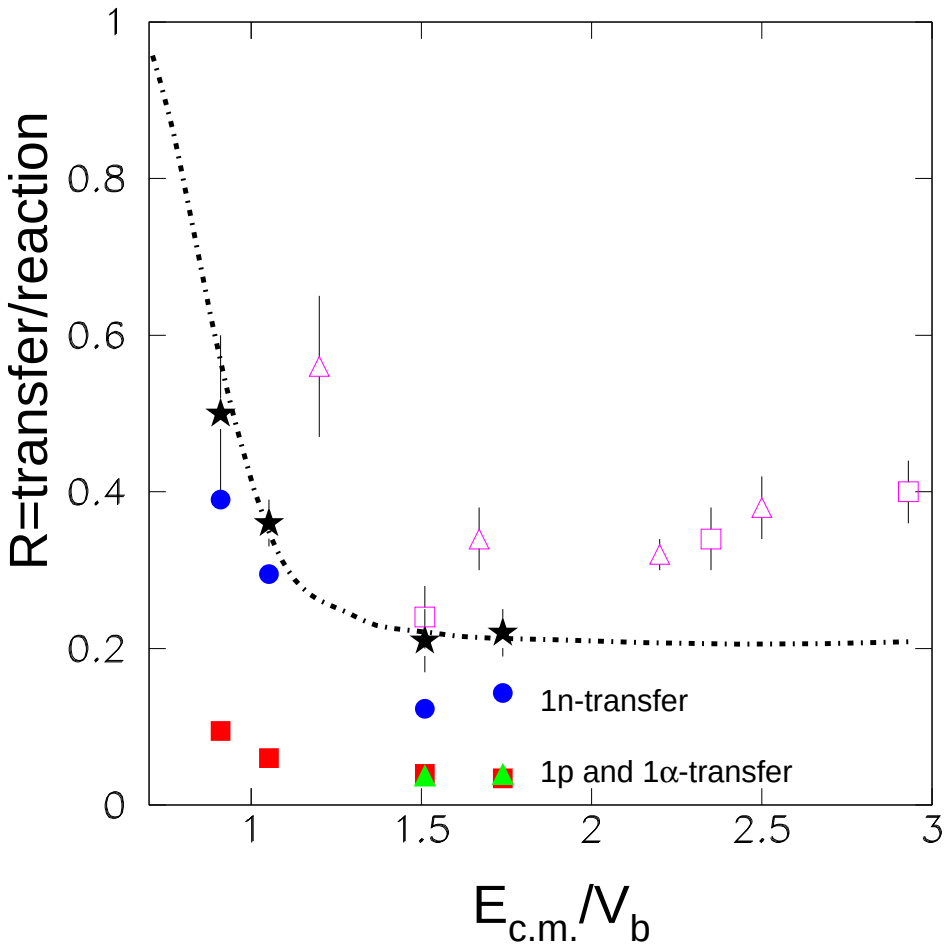

FIG. 3: Experimental ratios (R) of transfer versus total reaction cross sections obtained in the present work and in [18], represented with the stars are compared with theoretical calculations (dotted-dashed line) explained in the text. Also the decomposition of this transfer ratios, to 1n-transfer, designated with the sold circles, 1p-transfer designated with the solid cubes and 1α-transfer designated with the solid triangles are also presented Finally previous data [15] are shown with open squares for the presently studied system and with open triangles for ^{9}Be+^{28}Si. Used barriers in the center of mass according to Broglia [29] are Vb=7.03 and 9.08 MeV for ^{6}Li and ^{9}Be correspondingly.

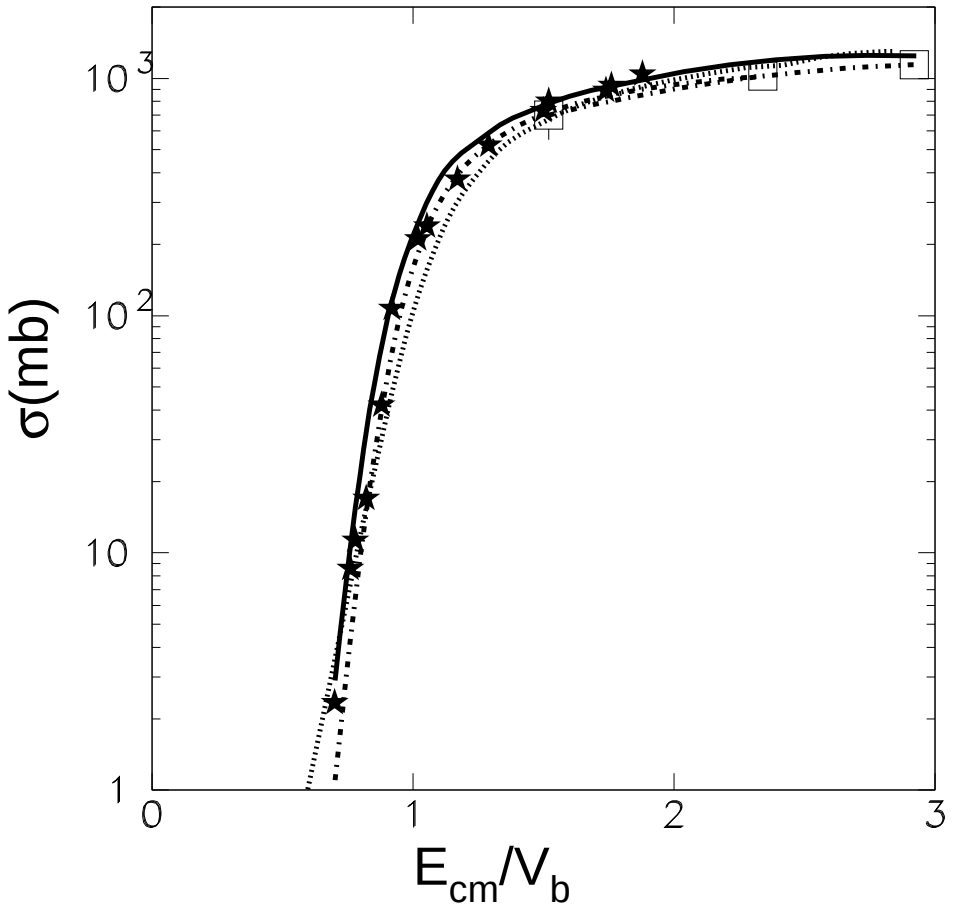

FIG. 4: Fusion measurements are compared with various BPM calculations according to: a) Wong (dotted line), b) ECIS calculations (dot-dashed line) and c) CDCC+BPM calculations (solid line). Previous fusion cross sections [15] at much higher energies than the Coulomb barrier namely E_{lab}= 13, 20 and 25 MeV, are also presented with open squares and show fair agreement with the present data, exhibiting lower strengths.

.